

Quantum echo in two-component Bose-Einstein condensates

Chang-Yan Wang ^{*}

Institute for Advanced Study, Tsinghua University, Beijing 100084, China



(Received 25 February 2024; accepted 5 June 2024; published 24 June 2024)

The development of ultracold atom technology has enabled precise investigations on the quantum dynamics of quantum gases. Recently, inspired by experimental advancement, the $SU(1, 1)$ echo, akin to the well-known $SU(2)$ spin echo, was proposed for the single-component Bose-Einstein condensate (BEC). In this paper, we investigate the possibility of quantum echo in the more intricate two-component BEC by fully exploiting its underlying symmetry, which is the Lie group $Sp(4, R)$. We demonstrate that quantum echo can occur for the two-component BEC by applying a driving protocol consisting of two steps in each period. The first step can be any Bogoliubov Hamiltonian, while the second step is a Hamiltonian with interactions turned off, which plays a similar role as the π pulse in spin echo. We confirm our theoretical results with numerical calculations for different examples of the two-component BEC. We further consider the effect of interactions between the excited boson modes on the quantum echo process and discuss the possible experimental implementation of this quantum echo.

DOI: [10.1103/PhysRevA.109.063327](https://doi.org/10.1103/PhysRevA.109.063327)

I. INTRODUCTION

In the past decades, ultracold-atomic systems have emerged as a powerful tool for the precise exploration of dynamics within quantum systems as they offer high controllability and tunability [1–3]. Recently, the Chicago group's experiments on Bose-Einstein condensates (BECs) revealed exotic phenomena like Bose fireworks and the quantum revival of BEC [4–12]. The second of these inspired the study of the quantum echo, i.e., the revival of the quantum state of a system after applying a specific driving protocol in the single-component BEC using the $SU(1, 1)$ group [13–17], which resembles the $SU(2)$ spin echo [18].

However, BEC can also form in more complex systems consisting of two or more species (internal states) of bosonic atoms, such as the two-component and spinor BECs [19–21]. The two-component BEC has been realized in various ultracold atom systems [22–33] and received extensive investigations [34–45]. Given the tunability of the interaction between different species of atoms through Feshbach resonances [27], one may wonder whether such a quantum echo can occur in this more complicated two-component BEC system.

In this paper, we address this problem by using the general formalism presented in Ref. [46], which employed the so-called real symplectic group $Sp(4, R)$ to deal with the quantum dynamics of the two-component BEC. The $Sp(4, R)$ group, a noncompact Lie group, preserved the canonical commutation relations of boson operators [47] and finds applications across various areas of physics, such as quantum information [48–50], high energy physics [51–54], and cold atoms [46,55–57]. (See Appendix A for a brief introduction

to this group.) In Ref. [46], by mapping the time evolution operator of BEC to an $Sp(4, R)$ matrix, the quantum dynamics under arbitrary Bogoliubov Hamiltonian were calculated.

Utilizing this formalism, we show that, through a two-step periodic driving protocol, the fully condensed state or any $Sp(4, R)$ coherent state of a two-component BEC can revert to its original form after two driving periods. The first-step Hamiltonian \hat{H}_1 can be any Bogoliubov Hamiltonian, while in the second step \hat{H}_2 the interactions are turned off. We provide a method to calculate \hat{H}_2 for a given \hat{H}_1 . This is demonstrated through two examples: a time-independent \hat{H}_1 and a time-dependent \hat{H}_1 , with numerical results confirming our theory. We also examine the quantum echo breaking effect due to interactions between excited boson modes and analyze how this effect varies with the kinetic to interaction strength ratio in the first-step Hamiltonian. The paper concludes with a discussion on the potential implementations of these quantum echoes in cold atom experiments.

Our work highlights the exploitation of the underlying symmetry of the two-component BEC. Since it has similar symmetry properties shared by the N -component BEC, our work provides a unified perspective on the quantum echoes of one- and two-component BECs, and can be potentially generalized to the spinor BEC case. Furthermore, given the presence of real symplectic groups in various areas of physical study [49–57], especially the bosonic Gaussian states [48], our work can shed light on the revival of quantum states in these research areas.

This paper is organized as follows. In Sec. II, we review the formalism using the $Sp(4, R)$ group to deal with the quantum dynamics of two-component BEC. In Sec. III, we prove that a two-step driving protocol can make the quantum echo occur. In Sec. IV, we apply this driving protocol to two different examples and present the numerical results to confirm our proof. In Sec. V, we consider the interaction effect. In Sec. VI,

^{*}Contact author: changyanwang@tsinghua.edu.cn

we propose a possible experimental implementation of this echo. We conclude in Sec. VII.

II. QUANTUM DYNAMICS AND $\text{Sp}(4, R)$ SYMMETRY

We consider the physical process that a two-component Bose gas is prepared in a fully condensed state, i.e., all particles are condensed in the zero momentum modes, then the system evolves under the Bogoliubov Hamiltonian. The general form of this quench Bogoliubov Hamiltonian can be written as $\hat{H}_{\text{Bg}}(t) = \sum_{\mathbf{k} \neq \mathbf{0}} \hat{H}_{\mathbf{k}}(t) + \text{const.}$, where

$$\hat{H}_{\mathbf{k}}(t) = \hat{\Psi}_{\mathbf{k}}^\dagger \mathcal{H}_{\mathbf{k}}(t) \hat{\Psi}_{\mathbf{k}}, \quad \mathcal{H}_{\mathbf{k}}(t) = \begin{pmatrix} \xi_{\mathbf{k}}(t) & \eta(t) \\ \eta^*(t) & \xi_{\mathbf{k}}^*(t) \end{pmatrix}, \quad (1)$$

with $\hat{\Psi}_{\mathbf{k}} = (a_{1,\mathbf{k}}, a_{2,\mathbf{k}}, a_{1,-\mathbf{k}}^\dagger, a_{2,-\mathbf{k}}^\dagger)^T$ [46,58]. Here $\xi_{\mathbf{k}}(t)$ is a 2×2 Hermitian matrix given by $\xi_{\mathbf{k},ij}(t) = \frac{1}{2}[\varepsilon_{\mathbf{k},ij}(t) + g_{ij}(t)\psi_i\psi_j^*]$ and $\eta(t)$ is a complex symmetric matrix given by $\eta_{ij}(t) = \frac{1}{2}g_{ij}(t)\psi_i\psi_j$, and $i, j = 1, 2$ labels the two species of bosons. The diagonal elements of $\varepsilon_{\mathbf{k}}(t)$ are the kinetic terms, whereas the off-diagonal elements are the spin-orbit coupling terms. $g_{ij}(t)$ represents the intra and interspecies interaction strengths of these two species of bosons. $\psi_i = \sqrt{N_i/V}e^{i\theta}$ are the condensate wave functions of the zero momentum modes. For simplicity, we set $\hbar = 1$.

However, the two species of the boson operators naturally give a representation of the Lie algebra of the real symplectic group $\text{Sp}(4, R)$ [47,59]. The generators of this Lie algebra can be defined as

$$\begin{aligned} \hat{\mathcal{X}}_{ij} &= a_{i,\mathbf{k}}a_{j,-\mathbf{k}} + a_{j,\mathbf{k}}a_{i,-\mathbf{k}}, \\ \hat{\mathcal{X}}^{ij} &= a_{i,\mathbf{k}}^\dagger a_{j,-\mathbf{k}}^\dagger + a_{j,\mathbf{k}}^\dagger a_{i,-\mathbf{k}}^\dagger, \\ \hat{\mathcal{X}}_l^k &= a_{k,\mathbf{k}}^\dagger a_{l,\mathbf{k}} + a_{l,-\mathbf{k}} a_{k,-\mathbf{k}}^\dagger, \end{aligned} \quad (2)$$

where $i, j, k, l = \{1, 2\}$, and ten of them are independent. The Casimir operator of this Lie algebra is given by [59]

$$\mathcal{C} = \hat{\mathcal{X}}^{ij} \hat{\mathcal{X}}_{ij} + \hat{\mathcal{X}}_{ij} \hat{\mathcal{X}}^{ij} - 2\hat{\mathcal{X}}_i^i \hat{\mathcal{X}}_j^j. \quad (3)$$

To show that this is a conserved quantity, we can rewrite it as [59]

$$\mathcal{C} = -2(\Delta N_{\mathbf{k}} + 2)(\Delta N_{\mathbf{k}} - 2), \quad (4)$$

where $\Delta N_{\mathbf{k}} = \sum_{i=1}^2 (a_{i,\mathbf{k}}^\dagger a_{i,\mathbf{k}} - a_{i,-\mathbf{k}}^\dagger a_{i,-\mathbf{k}})$ counts the difference in the number of bosons between the momenta $+\mathbf{k}$ and $-\mathbf{k}$. According to the definition of $\mathfrak{sp}(4, R)$ generators Eq. (2), none of these generators change this number difference. Thus, the Casimir operator is conserved.

These operators have a one-to-one correspondence with the matrix representation of the $\mathfrak{sp}(4, R)$ Lie algebra. This correspondence can be revealed by rewriting the operators defined in Eq. (2) as

$$\hat{\mathcal{X}}_{ij} = \hat{\Psi}_{\mathbf{k}}^\dagger \kappa Y_{ij} \hat{\Psi}_{\mathbf{k}}, \quad \hat{\mathcal{X}}^{ij} = \hat{\Psi}_{\mathbf{k}}^\dagger \kappa Y^{ij} \hat{\Psi}_{\mathbf{k}}, \quad \hat{\mathcal{X}}_l^k = \hat{\Psi}_{\mathbf{k}}^\dagger \kappa Y_l^k \hat{\Psi}_{\mathbf{k}}, \quad (5)$$

where $\kappa = \text{diag}(1, 1, -1, -1)$ [46,59]. Here, these 4×4 matrices $\{Y_{ij}, Y^{ij}, Y_l^k\}$ are the matrix representation of the Lie algebra $\mathfrak{sp}(4, R)$, and their explicit form is given in Appendix B. Then, we can write the Bogoliubov Hamiltonian

$\hat{H}_{\mathbf{k}}$ in terms of these generators as

$$\hat{H}_{\mathbf{k}}(t) = \xi_{\mathbf{k},ij}(t) \hat{\mathcal{X}}_j^i + \frac{1}{2} \eta_{ij}(t) \hat{\mathcal{X}}_{ij} + \frac{1}{2} \eta_{ij}^*(t) \hat{\mathcal{X}}^{ij}, \quad (6)$$

where we adopt the Einstein summation convention, i.e., the repeated indices i and j are summed over. In the following, we always adopt this convention implicitly. Hence, the time evolution operator

$$\hat{U}_{\mathbf{k}}(t) = \mathcal{T} e^{-i \int_0^t \hat{H}_{\mathbf{k}}(t') dt'} \quad (7)$$

gives a representation of the real symplectic group $\text{Sp}(4, R)$, i.e., $\hat{U}_{\mathbf{k}}(t)$ has a one-to-one correspondence to a matrix in the group $\text{Sp}(4, R)$, which is given by

$$U_{\mathbf{k}}(t) = \mathcal{T} e^{-i \int_0^t \kappa \mathcal{H}_{\mathbf{k}}(t') dt'}. \quad (8)$$

Here, \mathcal{T} is the time-ordering operator. This can be seen by noticing that the matrix corresponding to the operator $\hat{H}_{\mathbf{k}}(t)$ is

$$\kappa \mathcal{H}_{\mathbf{k}}(t) = \xi_{\mathbf{k},ij}(t) Y_j^i + \frac{1}{2} \eta_{ij}(t) Y_{ij} + \frac{1}{2} \eta_{ij}^*(t) Y^{ij}.$$

Since the matrix $U_{\mathbf{k}}(t)$ is a real symplectic matrix, it has the form [47]

$$U_{\mathbf{k}}(t) = \begin{pmatrix} \mathcal{U}(t) & \mathcal{V}(t) \\ \mathcal{V}(t)^* & \mathcal{U}(t)^* \end{pmatrix}, \quad (9)$$

where $\mathcal{U}(t), \mathcal{V}(t)$ are 2×2 matrices satisfying

$$\mathcal{U}(t)\mathcal{U}(t)^\dagger - \mathcal{V}(t)\mathcal{V}(t)^\dagger = I, \quad \mathcal{U}(t)\mathcal{V}(t)^T = \mathcal{V}(t)\mathcal{U}(t)^T. \quad (10)$$

To calculate the time evolution of the fully condensed state, one can decompose $\hat{U}_{\mathbf{k}}(t)$ as

$$\hat{U}_{\mathbf{k}}(t) = e^{-\frac{1}{2} Z_{ij}(t) \hat{\mathcal{X}}^{ij}} e^{\zeta_{kl}(t) \hat{\mathcal{X}}_l^k} e^{-\frac{1}{2} v_{ij}(t) \hat{\mathcal{X}}_{ij}}, \quad (11)$$

which is called normal order decomposition [46,47]. With this decomposition, the fully condensed state $|\mathbf{0}\rangle$ evolves as

$$\hat{U}_{\mathbf{k}}(t)|\mathbf{0}\rangle = \mathcal{N}_{\mathbf{k}} e^{-\frac{1}{2} Z_{ij}(t) \hat{\mathcal{X}}^{ij}} |\mathbf{0}\rangle \equiv |Z(t)\rangle, \quad (12)$$

where $|Z(t)\rangle$ is an $\text{Sp}(4, R)$ coherent state and $\mathcal{N}_{\mathbf{k}}$ is the normalization factor. At any time t of the evolution, $Z(t)$ is [46,60]

$$Z(t) = \mathcal{V}(t)[\mathcal{U}(t)^*]^{-1}, \quad (13)$$

where $\mathcal{U}(t), \mathcal{V}(t)$ is defined in Eq. (9). By using Eq. (10), it can be shown that at any time t , $Z(t)$ is a 2×2 symmetric complex matrix and $I - Z(t)^\dagger Z(t)$ is positive definite, where I is 2×2 identity matrix. Thus, the matrix $Z(t)$ can be parameterized by three complex numbers $Z_{11}(t), Z_{12}(t), Z_{22}(t)$, or by six real parameters. Mathematically, $Z(t)$ lies in a six-dimensional manifold called Cartan classical domain, and is isomorphic to the quotient space $\text{Sp}(4, R)/U(2)$ [47,61], where $U(2)$ is the unitary group of degree 2. Thus, $Z(t)$ gives a trajectory in this six-dimensional manifold. In addition, if the initial state is the arbitrary coherent state $|Z_0\rangle$, the time evolution of this coherent state is also a coherent state, i.e., $\hat{U}_{\mathbf{k}}(t)|Z_0\rangle = |Z'(t)\rangle$, and $Z'(t)$ is given by [46,60]

$$Z'(t) = [\mathcal{U}(t)Z_0 + \mathcal{V}(t)][\mathcal{V}(t)^*Z_0 + \mathcal{U}(t)^*]^{-1}. \quad (14)$$

With this general formalism dealing with the time evolution of two-component BEC in hand we are ready to study the quantum echo of the two-component BEC system.

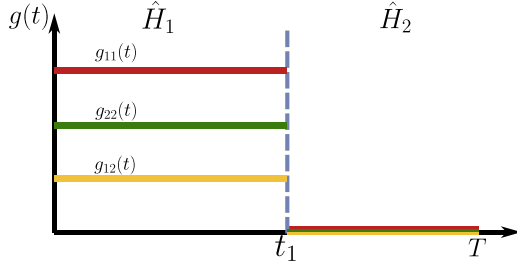


FIG. 1. Schematics for the driving protocol. In the first step of a period, the Hamiltonian can be any Bogoliubov Hamiltonian. However, in the second step of a period, all the interaction strengths should be turned off.

III. QUANTUM ECHO

In this section, we will study the problem of quantum echo for boson modes in generic $\pm \mathbf{k} \neq \mathbf{0}$ momenta by considering a periodic driving protocol similar to that found in Refs. [13,15]. In this driving protocol, each period consists of two steps: in the first step, the Hamiltonian \hat{H}_1 is a generic two-component Bogoliubov Hamiltonian defined in Eq. (6); in the second step, the Hamiltonian \hat{H}_2 only includes these $\hat{\mathcal{X}}_j^i$ operators, i.e., turning off all the intra and interspecies interaction strengths g_{ij} , as shown in Fig. 1. We will show how to obtain the explicit form of the second-step Hamiltonian \hat{H}_2 that makes the initial state, either $|\mathbf{0}\rangle$ or a generic coherent state $|Z_0\rangle$, reverse to itself after two period of driving for any given Bogoliubov Hamiltonian \hat{H}_1 .

In the m th period, when $(m-1)T < 0 \leq (m-1)T + t_1$, the Hamiltonian is

$$\hat{H}_1 = \xi_{ij}(t)\hat{\mathcal{X}}_j^i + \frac{1}{2}\eta_{ij}(t)\hat{\mathcal{X}}_{ij} + \frac{1}{2}\eta_{ij}^*(t)\hat{\mathcal{X}}^{ij}, \quad (15)$$

and when $(m-1)T + t_1 < t \leq mT$,

$$\hat{H}_2 = \frac{1}{2}\varepsilon_{ij}\hat{\mathcal{X}}_j^i, \quad (16)$$

where $T = t_1 + t_2$ is the duration of each period. Here we omit the subscript \mathbf{k} for simplicity. Thus, for such a quantum echo to occur, we require that the time evolution operators $\hat{U}_1(t_1)$ and $\hat{U}_2(t_2)$ of these two steps acting on any coherent state $|Z_0\rangle$ give

$$[\hat{U}_2(t_2)\hat{U}_1(t_1)]^2|Z_0\rangle = |Z_0\rangle. \quad (17)$$

According to Eq. (14), this condition is equivalent to

$$U(T)^2 = [U_2(t_2)U_1(t_1)]^2 = \pm 1, \quad (18)$$

where $U_i(t_i)$, $i = 1, 2$ are the time evolution matrix corresponding to $\hat{U}_i(t_i)$. Next we will focus on the case of $U(T)^2 = -1$ since the result for $U(T)^2 = 1$ case can be obtained by redefined $U(T)^2$ from the $U(T)^2 = -1$ case as $U(T)$.

Since $U(T)$ is also a real symplectic matrix, i.e., having the form of Eq. (9), substituting its elements \mathcal{U}, \mathcal{V} into Eq. (18) leads to

$$\begin{aligned} U^2 + \mathcal{V}\mathcal{V}^* &= U^{*2} + \mathcal{V}^*\mathcal{V} = -1, \\ \mathcal{U}\mathcal{V} + \mathcal{V}\mathcal{U}^* &= 0. \end{aligned} \quad (19)$$

By using the property of the real symplectic matrix $\mathcal{U}\mathcal{U}^\dagger - \mathcal{V}\mathcal{V}^\dagger = I$, $\mathcal{U}\mathcal{V}^T = \mathcal{V}\mathcal{U}^T$, Eqs. (19) result in

$$\mathcal{U} = -\mathcal{U}^\dagger. \quad (20)$$

This is the condition that $U(T)$ should satisfy for the quantum echo to occur.

Next, we will construct an explicit form of $U(T)$. We recall that for the $SU(1, 1)$ case, an $SU(1, 1)$ matrix satisfying $U^2 = -1$ can be given by

$$\left(e^{i\pi\frac{\alpha_\pm}{2}}e^{i(\alpha_+\sigma^+ - \alpha_-\sigma^-)}\right)^2 = -1, \quad (21)$$

where $\{\sigma_z/2, \sigma^+, -\sigma^-\}$ are the generators of the $SU(1, 1)$ group, with $\sigma_{x,y,z}$ the Pauli matrices and $\sigma^\pm = 1/2(\sigma_x \pm i\sigma_y)$, and α_\pm are arbitrary complex numbers. We notice the resemblance in form between $\{\sigma_z, \sigma^+, -\sigma^-\}$ and $\{Y_i^k, Y_{ij}, Y^{ij}\}$. Inspired by this resemblance, we expect that, for the $Sp(4, R)$ case, the matrix $U(T)$ satisfying $U(T)^2 = -1$ is given by

$$U(T) = e^{i\frac{\pi}{2}(Y_1^1 + Y_2^2)}e^{\frac{1}{2}(\eta_{ij}Y^{ij} + \eta_{ij}^*Y_{ij})} \quad (22)$$

where η is a 2×2 symmetric complex matrix. Since $e^{i\frac{\pi}{2}(Y_1^1 + Y_2^2)} = \text{diag}(i, i, -i, -i)$, substituting the above equation to Eq. (20) leads to the fact that the submatrix \mathcal{U}_0 of $U_0 = e^{\frac{1}{2}(\eta_{ij}Y^{ij} + \eta_{ij}^*Y_{ij})}$ should be Hermitian, i.e., $\mathcal{U}_0 = \mathcal{U}_0^\dagger$. In Appendix B, we give the explicit expression of \mathcal{U}_0 and also prove that \mathcal{U}_0 is Hermitian. As a result, we prove that the form of $U(T)$ given in Eq. (22) actually satisfies $U(T)^2 = -1$.

With the general form of $U(T)$, we can find the \hat{H}_2 that make the quantum echo occur for arbitrary \hat{H}_1 . Since \hat{H}_1 is of the general form of Eq. (6), its corresponding time evolution matrix is also of the general form of real symplectic matrix Eq. (9), i.e.,

$$U_1(t_1) = \begin{pmatrix} \mathcal{U}_1(t_1) & \mathcal{V}_1(t_1) \\ \mathcal{V}_1(t_1)^* & \mathcal{U}_1(t_1)^* \end{pmatrix}. \quad (23)$$

However, \hat{H}_2 only has $\hat{\mathcal{X}}_j^i$ terms, thus, its corresponding time evolution matrix is block diagonal, i.e.,

$$U_2(t_2) = \begin{pmatrix} \mathcal{U}_2(t_2) & 0 \\ 0 & \mathcal{U}_2(t_2)^* \end{pmatrix}. \quad (24)$$

The constraints on the real symplectic matrix Eq. (10) also results in that $\mathcal{U}_2(t_2)$ is unitary. Then, by substituting the elements of $U_1(t_1)$ and $U_2(t_2)$ into $U(T) = U_2(t_2)U_1(t_1)$, we have

$$-i\mathcal{U}_1(t_1) = \mathcal{U}_2(t_2)^{-1}\mathcal{U}_0. \quad (25)$$

Since we show that $\mathcal{U}_2(t_2)^{-1}$ is unitary and \mathcal{U}_0 is Hermitian, the right-hand side of the above equation is just the polar decomposition of $-i\mathcal{U}_1(t_1)$. The polar decomposition of a complex matrix is the factorization of this matrix into a product of unitary matrix and a Hermitian matrix. In addition, the polar decomposition of a square matrix always exists. Hence, by performing the polar decomposition we can find $\mathcal{U}_2(t_2)$. The explicit form of \mathcal{H}_2 is given by

$$\mathcal{H}_2 = \kappa \ln[\mathcal{U}_2(t_2)]/(-it_2), \quad (26)$$

where $\kappa = \text{diag}(1, 1, -1, -1)$.

To have a better understanding of why we choose $U(T)$ to have the form of Eq. (22), we can let $\hat{H}_1 = -\frac{1}{2}(\eta_{ij}\hat{\mathcal{X}}^{ij} +$

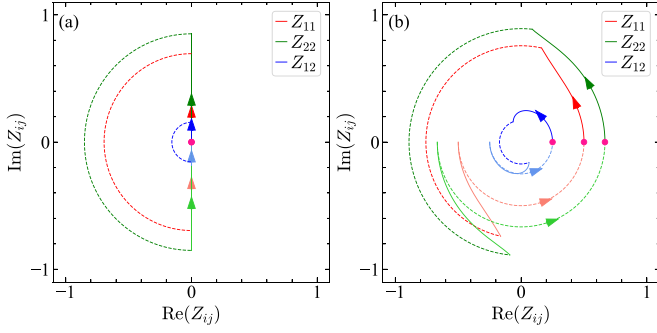


FIG. 2. Trajectories of the elements of $Z(t)$ when $\eta_{11} = 1$, $\eta_{22} = 3/2$, $\eta_{12} = 1/2$ for when (a) the initial state is $|\mathbf{0}\rangle$ and (b) the initial state is a coherent state $|Z_0\rangle$ with $Z_0 = \begin{pmatrix} 1/2 & 1/4 \\ 1/4 & 2/3 \end{pmatrix}$. The evolution includes two periods. The lines (both solid and dashed) with darker colors represent the first period and the line with lighter colors represent the second period. The solid lines represent the first steps and the dashed lines represent the second steps.

$\eta_{ij}^* \hat{\chi}_{ij}$, $\hat{H}_2 = -\frac{\pi}{2}(\hat{\chi}_1^2 + \hat{\chi}_2^2)$, and the times $t_1 = t_2 = 1$. Figure 2 shows the trajectory of the elements of the matrix Z_t in the complex plane for the cases when the initial state is $|\mathbf{0}\rangle$ and a generic coherent state $|Z_0\rangle$, respectively. It can be seen that, in both cases, all the trajectories perfectly return to their initial points, which confirms the above proof. From this figure, we can see that, for both cases, the second step \hat{H}_2 amounts to a π rotation for all the elements of the Z_t matrix. It reverses the direction of the trajectories and makes the trajectories return to their initial points. Thus, we can see that the second-step Hamiltonian plays a similar role to the π pulse in the SU(2) spin echo. Meanwhile, when the initial state is $|\mathbf{0}\rangle$, the second step in the second period is not necessary for quantum echo, and applying \hat{H}_1 , \hat{H}_2 , and \hat{H}_1 in consequence suffices to make the state return to its initial state. However, if the initial state is a generic coherent state, the fully driven protocol is necessary for the quantum echo to occur.

IV. NUMERICAL RESULTS

In the previous section, we provide a protocol that can bring any coherent state back to itself after two periods of driving for any Bogoliubov Hamiltonian \hat{H}_1 . Briefly, in this

protocol, each period consists of two steps: the first step can be any Bogoliubov Hamiltonian \hat{H}_1 and the second step is a quadratic Hamiltonian \hat{H}_2 with all interaction strengths turned off. The Hamiltonian in the second step can be found by performing a polar decomposition for the 2×2 submatrix of the time evolution matrix $U_1(t_1)$ as shown in Eqs. (25) and (26).

In this section, we will apply this protocol to some examples and present the numerical results. The first example is the case when the interaction strengths all remain constant in the first step of a period as shown in Fig. 3. For simplicity, in the first step of each driving period we set the masses of the two species of bosons equal and set the spin-orbit coupling as 0, more specifically, we set $\varepsilon_{\mathbf{k}} = \text{diag}(\varepsilon_0, \varepsilon_0)$, where the matrix $\varepsilon_{\mathbf{k}}$ is defined in Eq. (1). Here, $\varepsilon_0 = \mathbf{k}^2/2m_1$ is the kinetic energy of the first boson mode and serves as an energy unit. Although we set the boson masses equal for simplicity, our approach also applies to the general case with unequal boson masses, as demonstrated analytically in the previous section. In addition, the interaction terms η_{ij} are chosen as $\eta_{11} = 1.25\varepsilon_0$, $\eta_{22} = \varepsilon_0$, $\eta_{12} = 0.5\varepsilon_0$ as shown in Fig. 3(a). We also choose the duration of each step equal, i.e., $t_1 = t_2 = 1/\varepsilon_0$. According to Eqs. (25) and (26), the Hamiltonian in the second step is

$$\mathcal{H}_2 = \begin{pmatrix} \varepsilon & 0 \\ 0 & \varepsilon^* \end{pmatrix}, \quad \varepsilon \simeq -\begin{pmatrix} 2.85 & 0.21 \\ 0.21 & 2.75 \end{pmatrix} \varepsilon_0. \quad (27)$$

Here, we can see that with the interaction strengths turned off, only the kinetic terms and the spin-orbit coupling terms remain in \mathcal{H}_2 . However, the diagonal terms in ε are no longer equal, which means different chemical potentials for these two species of bosons are required. Meanwhile, the off-diagonal terms are also no longer 0, requiring nonzero spin-orbit coupling.

The numerical results for this case are shown in Fig. 3. Figure 3(a) shows the values of the interaction strengths. Figure 3(b) shows the evolution of the three independent complex elements of the symmetric matrix $Z(t)$ in the complex plane when the initial state is the fully condensed state $|\mathbf{0}\rangle$. In Fig. 3(c), we show the evolution of the particle number of each component of the boson, which can be calculated by using the method presented in Ref. [46]. Figures 3(d) and 3(e) show the trajectories and particle numbers when the initial state is a generic nonvacuum coherent state.

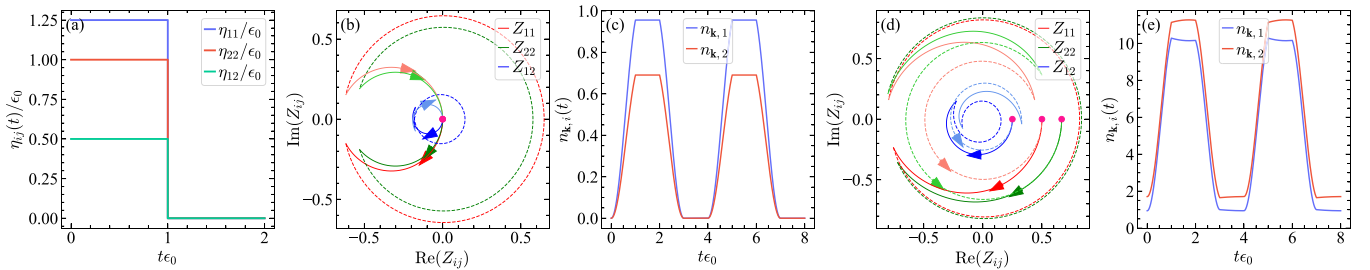


FIG. 3. Quantum echo when the interaction strengths are all constant in the first step of each period. (a) The interaction terms $\eta_{ij}(t)$ in one period. (b) The trajectory of the $Z(t)$ matrix in the parameter space when initial state is $|\mathbf{0}\rangle$. The purple dot represents the initial state and the arrows represent the direction of the trajectories as time evolves. The solid lines represent the first step and the dashed lines represent the second step. The lines with deep colors are the first period and the light-colored ones represent the second period. (c) The time evolution of the particle number for each species of bosons when initial state is a vacuum. (d,e) the same Hamiltonian as (c,d), but the initial is a generic coherent state $|Z_0\rangle$ which is the same as the one in Fig. 2.

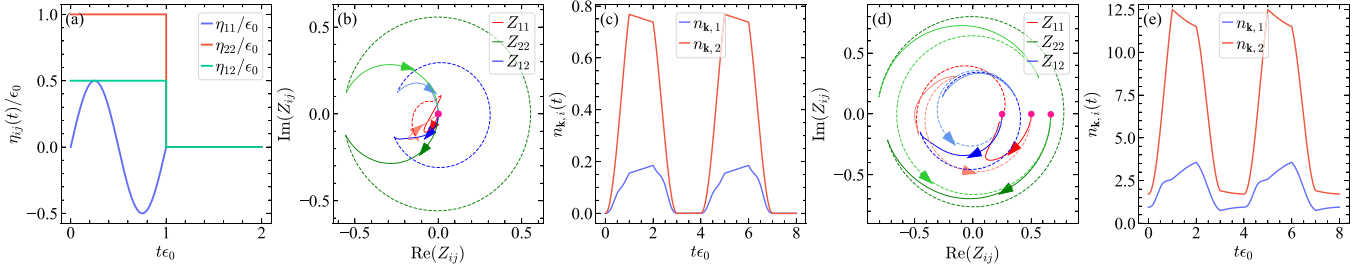


FIG. 4. Quantum echo when one interaction strength is a sine wave. (a) The interactions $g_{ij}(t)$ in a period. (b) The trajectory of the $Z(t)$ matrix in the parameter space when initial state is the vacuum. The convention in this figure is the same as Fig. 3. (c) The time evolution of the particle number of each species of bosons when initial state is a vacuum. (d), (e) The same Hamiltonian as (c), (d), but the initial is a generic coherent state $|Z_0\rangle$, which is the one we use in Fig. 2.

The second example is the case when one of the interaction strengths is a sine wave in the first step of each period as shown in Fig. 4. Here, we still choose the $\varepsilon_{\mathbf{k}}$ matrix in the first-step Hamiltonian as diagonal, i.e., $\varepsilon_{\mathbf{k}} = \text{diag}(\varepsilon_0, \varepsilon_0)$, and set the duration of each step equal i.e., $t_1 = t_2 = 1/\varepsilon_0$. For the interaction terms, $\eta_{11} = \varepsilon_0 \sin(2\pi\varepsilon_0 t)/2$, $\eta_{22} = \varepsilon_0$, and $\eta_{12} = 0.5\varepsilon_0$, as shown in Fig. 4. Using the same procedure, we can calculate the second-step Hamiltonian $\mathcal{H}_2 = \text{diag}(\varepsilon, \varepsilon^*)$, where

$$\varepsilon \simeq - \begin{pmatrix} 2.02 & 0.36 - 0.009i \\ 0.36 + 0.009i & 2.73 \end{pmatrix} \varepsilon_0. \quad (28)$$

In Fig. 4, we show the evolution trajectories in the parameter space and the evolution of particle numbers when the initial state is a fully condensed state and a generic coherent state.

From the numerical results present in Figs. 3 and 4, we can see that our formalism can clearly display how the initial state evolves in the entire driving process. It is clearly shown that, for these two examples, the driving protocol can bring both the fully condensed state and a generic coherent state back to themselves after two periods. Meanwhile, in these examples, the trajectories of the case with a generic coherent state as the initial state are more complicated than the case with a fully condensed state as initial state. Furthermore, we also show the time evolution of the particle numbers of the two species of bosons. The particle numbers increase rapidly in the first step of the first period, and then in the second step they cease to grow. In the first step of the second period, the particle numbers start to decrease. Finally, they return to their initial values. Thus, the numerical results clearly demonstrate how the quantum echo happens in the two-component BEC systems.

V. INTERACTION EFFECT

In this section, we will consider the interaction effect in the quantum echo process. Similar to the one-component BEC [15], the interaction between these boson modes in two-component BEC can be given as $\hat{V} = \sum_{i,j} (4\hat{n}_{i,\mathbf{k}}\hat{n}_{j,-\mathbf{k}} + \hat{n}_{i,\mathbf{k}}\hat{n}_{j,\mathbf{k}} + \hat{n}_{i,-\mathbf{k}}\hat{n}_{j,-\mathbf{k}})$. When there is a large amount of boson modes excited in the $\pm\mathbf{k}$ momenta, the interaction between these excitations cannot be ignored. As a result, the quantum echo process will be broken. By calculating the particle numbers in the end of the $2m$ th period, we want to reveal the interplay of the interactions between boson modes and the

parameters in the original first-step Hamiltonian \hat{H}_1 in this quantum echo breaking process.

For simplicity, we consider the following two-step driving

$$\begin{aligned} \hat{H}'_1 &= \hat{H}_1 + \tilde{g}\hat{V}, \\ \hat{H}_2 &= \frac{1}{2}\varepsilon_{ij}\hat{\mathcal{X}}_j^i, \end{aligned} \quad (29)$$

where $\hat{H}_1 = (E\delta_{ij} + \gamma\eta_{ij})\hat{\mathcal{X}}_j^i + \frac{\gamma}{2}\eta_{ij}(\hat{\mathcal{X}}^{ij} + \hat{\mathcal{X}}_{ij})$. Here we assume the condensate wave functions $\psi_i = \sqrt{N_i/V}$ are real and δ_{ij} is the Kronecker delta. Thus, the parameter E controls the kinetic term and the dimensionless parameter γ controls the hopping between the excitations and the condensate in the zero momentum. The \hat{H}_2 is chosen such that when $\tilde{g} = 0$ the above driving process will bring the initial state to itself after two period of evolution.

When $\tilde{g} \neq 0$, and \tilde{g} is much smaller than the energy scale of \hat{H}_1 , we can treat the interaction term perturbatively. By keeping the Dyson series to the first order, we have

$$\begin{aligned} \hat{U}'_1 &= e^{-i\hat{H}'_1 t_1} \\ &= e^{-i\hat{H}_1 t_1} \left[1 - i\tilde{g} \int_0^{t_1} \hat{V}(t) dt + O(U^2) \right], \end{aligned} \quad (30)$$

where $\hat{V}(t) = e^{i\hat{H}_1 t} \hat{V} e^{-i\hat{H}_1 t}$. Since \hat{H}_1 is a linear combination of the $\mathfrak{sp}(4, R)$ Lie algebra, according to Refs. [46,47], the operator $\Psi_{\mathbf{k}}$ evolves as

$$e^{i\hat{H}_1 t} \Psi_{\mathbf{k}} e^{-i\hat{H}_1 t} = e^{-i\kappa\mathcal{H}_1 t} \Psi_{\mathbf{k}}. \quad (31)$$

With this transformation, $\hat{V}(t)$ can be calculated. Then, the time evolution operator after two period of driving up to the first order in \tilde{g} has the following form:

$$\begin{aligned} \hat{U}(2T) &= \hat{U}_2 \hat{U}'_1 \hat{U}_2 \hat{U}'_1 \\ &= \left[1 - i\tilde{g} \int_0^{t_1} dt \hat{A} \hat{V}(t) \hat{A}^\dagger \right. \\ &\quad \left. - i\tilde{g} \int_0^{t_1} dt \hat{A}^2 \hat{V}(t) (\hat{A}^\dagger)^2 + O(\tilde{g}^2) \right] \hat{A}^2 \\ &\equiv [1 - i\tilde{g}\hat{\mathcal{V}} + O(\tilde{g}^2)] \hat{A}^2, \end{aligned} \quad (32)$$

where we define $\hat{A} = e^{-i\hat{H}_2 t_2} e^{-i\hat{H}_1 t_1}$, and denote the integral terms as $\hat{\mathcal{V}}$. Here, $\hat{A} \hat{V}(t) \hat{A}^\dagger$ and $\hat{A}^2 \hat{V}(t) (\hat{A}^\dagger)^2$ can also be calculated using the method in Eq. (31). As a result, the particle

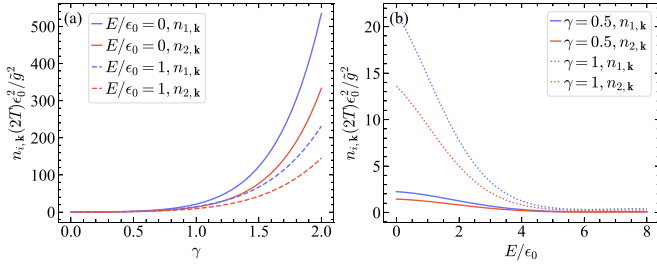


FIG. 5. Particle numbers at the end of the $2T$ for each species of boson with (a) varying γ and (b) varying E . For all these cases, the matrix $\eta = \begin{pmatrix} 1/2 & 1/6 \\ 1/6 & 1/4 \end{pmatrix} \epsilon_0$, where $\epsilon_0 = 2\eta_{11}$ serves as an energy unit.

number at the end of the $2m$ th period is given by

$$\begin{aligned} n_{i,\mathbf{k}}(2mT) &= \langle 0 | [\hat{U}^\dagger(2T)]^m \hat{n}_{i,\mathbf{k}} [\hat{U}(2T)]^m | 0 \rangle \\ &= m^2 \tilde{g}^2 \langle 0 | \hat{\mathcal{V}}^\dagger \hat{n}_{i,\mathbf{k}} \hat{\mathcal{V}} | 0 \rangle + O(\tilde{g}^3), \end{aligned} \quad (33)$$

where $\hat{n}_{i,\mathbf{k}} = a_{i,\mathbf{k}}^\dagger a_{i,\mathbf{k}}$. Here, we use the relations $\hat{A}^2 | 0 \rangle = -| 0 \rangle$ and $\hat{A}^2 \hat{n}_{i,\mathbf{k}} (\hat{A}^\dagger)^2 = \hat{n}_{i,\mathbf{k}}$. Then, the expectation value part of the above expression can be evaluated numerically. In addition, we can conclude that to the leading order, the particle numbers increase quadratically with interaction strengths \tilde{g} .

In Fig. 5, we show the numerical results for the particle numbers $n_{i,\mathbf{k}}(2T)$ at the end of the second driving period varying with the parameters E and γ with η_{ij} fixed. From Fig. 5(a), we can see that for different fixed values of E , the particle numbers increase exponentially with increasing γ . However, the particle numbers decrease as the parameter E increases. This result can be understood as follows: γ controls the hopping between the excitations and the condensate in zero momentum. When increasing γ with fixed kinetic term parameter E , more particles will be excited since the echo-breaking interactions are between the excited particles. Thus, more excited particles will result in a stronger echo-breaking effect. However, when increasing E with fixed γ , the ratio γ/E gets smaller, thus, the particles' exciting is suppressed. Hence, the echo-breaking effect is weaker in this case.

VI. POSSIBLE EXPERIMENTAL IMPLEMENTATION

In previous sections we explore a general driving protocol to facilitate quantum echo in two-component BECs and examine the influence of symmetry-breaking interactions on this phenomenon. In this section, we will propose a possible experiment implementation for this quantum echo.

The model in Eq. (1) involves the hopping between the bosonic modes in opposite momenta $\pm \mathbf{k}$. The similar hopping also appears in the single-component BEC case and is proposed to be implemented in a double-well structure in momentum space in Ref. [15]. This kind of double-well structure can be implemented in various experimental setups such as the shaken optical lattice, spin-orbit coupling, and periodic driving [15]. For the two-component case, we propose using a shaken optical lattice [62] setup. The experimental procedure would start with preparing a two-component BEC, initially condensing all particles in the zero momentum state. Subsequently, altering the band structure to form a double well

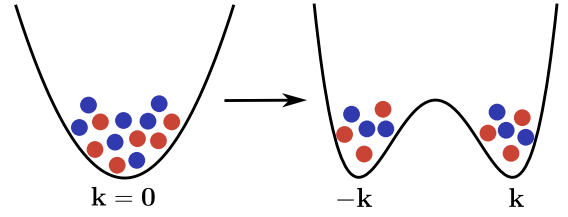


FIG. 6. Schematics for the shaken optical lattice implementation of hopping terms between opposite momenta of two-component BEC Hamiltonian. Red and blue dots represent two species of bosons.

would populate the particles in opposite momenta as shown in Fig. 6. This process corresponds to the hopping described in Eq. (1) from opposite momenta.

In the second step of our driving protocol, the coupling term between opposite momenta disappear, however, the spin-orbit coupling terms like $a_{i,\mathbf{k}}^\dagger a_{j,\mathbf{k}}$ with $i \neq j$ are always present. Importantly, the implementation of spin-orbit coupling is also feasible in cold atom experiments [63]. Therefore, the driving protocol we propose can be effectively realized within the current frameworks of cold atom experimental setups.

VII. CONCLUSION

In this paper we addressed the question of how quantum echo can be achieved in a two-component Bose-Einstein condensate system using the $\text{Sp}(4, R)$ group formalism. We showed that under a periodic driving protocol consisting of two steps in each period, any $\text{Sp}(4, R)$ coherent state of two-component BEC can reverse to itself after two periods of driving. We also developed a general method to construct the second-step Hamiltonian \hat{H}_2 from the first-step Hamiltonian \hat{H}_1 based on the property of real symplectic matrices and applied our method to two examples, one with time-independent \hat{H}_1 and one with time-dependent \hat{H}_1 , then verified our theoretical prediction numerically. Furthermore, we investigated how the interaction effect breaks the quantum echo process and found that the particle number deviation from the perfect revival is influenced by the ratio between the strengths of the kinetic terms and interaction in the first-step Hamiltonian \hat{H}_1 .

Our work extends the previous studies on quantum echo in single-component BEC and reveals additional features of two-component BEC dynamics. Our work also showcases the usefulness and elegance of the $\text{Sp}(4, R)$ group formalism for studying quantum systems with real symplectic structures. Since our proof on the occurrence of the quantum echo in two-component BEC system is solely based on the symplectic properties of the time evolution matrix, our result can also have potential use in the spinor BEC and N -component boson system. Meanwhile, given the presence of real symplectic matrices in various areas of physical study [48–57], we hope that our work will stimulate further research on this topic and inspire new applications of the quantum echo in ultracold atom systems and beyond.

ACKNOWLEDGMENTS

C.-Y.W. thanks Yan He for valuable discussions and suggestions on this manuscript. C.-Y.W. is supported by the Shuimu Tsinghua scholar program at Tsinghua University.

APPENDIX A: REAL SYMPLECTIC GROUP $\text{Sp}(2n, R)$

In this Appendix, we will give a brief introduction to the real symmetric group $\text{Sp}(2n, R)$, where n is a positive integer and R denotes the field of real numbers. When $n = 2$, we have the group $\text{Sp}(4, R)$. More details can be found in Ref. [59].

The real symplectic group $\text{Sp}(2n, R)$ is the set of $2n \times 2n$ real matrices preserving a nonsingular skew symmetric matrix Ω , i.e., for a real matrix $M \in \text{Sp}(2n, R)$, it satisfies

$$M^T \Omega M = \Omega, \quad (\text{A1})$$

where M^T is the transpose of M . Here, the matrix Ω is defined as

$$\Omega = \begin{pmatrix} 0 & I_n \\ -I_n & 0 \end{pmatrix}, \quad (\text{A2})$$

where I_n is the $n \times n$ identity matrix. Then, one can diagonalize the matrix Ω by a unitary transformation

$$U \Omega U^\dagger = i\kappa, \quad (\text{A3})$$

where κ is a diagonal matrix

$$\kappa = \begin{pmatrix} I_n & 0 \\ 0 & -I_n \end{pmatrix}, \quad (\text{A4})$$

and the unitary transformation U is given by

$$U = \frac{1}{\sqrt{2}} \begin{pmatrix} R & -iR \\ R & iR \end{pmatrix}, \quad (\text{A5})$$

where R is $n \times n$ matrix

$$R = \begin{pmatrix} 0 & 0 & \cdots & 0 & 1 \\ 0 & 0 & \cdots & 1 & 0 \\ \vdots & \vdots & 1 & \vdots & \vdots \\ 0 & 1 & \cdots & 0 & 0 \\ 1 & 0 & \cdots & 0 & 0 \end{pmatrix}. \quad (\text{A6})$$

Then, by substituting Eq. (A3) into Eq. (A1), we have

$$(UMU^\dagger)^\dagger \kappa (UMU^\dagger) = \kappa, \quad (\text{A7})$$

where we use the fact that M is a real matrix. Thus, by defining \mathcal{M} as

$$\mathcal{M} = UMU^\dagger, \quad (\text{A8})$$

we have another representation of the $\text{Sp}(2n, R)$ group. And \mathcal{M} satisfies the constraint

$$\mathcal{M}^\dagger \kappa \mathcal{M} = \kappa. \quad (\text{A9})$$

By substituting Eq. (A3) into Eq. (A7), we can see that the matrix \mathcal{M} has the form

$$\mathcal{M} = \begin{pmatrix} \mathcal{U} & \mathcal{V} \\ \mathcal{V}^* & \mathcal{U}^* \end{pmatrix}, \quad (\text{A10})$$

where \mathcal{U} and \mathcal{V} are $n \times n$ matrices. Thus the constraint in Eq. (A9) becomes

$$\mathcal{U}\mathcal{U}^\dagger - \mathcal{V}\mathcal{V}^\dagger = I_n, \quad \mathcal{U}\mathcal{V}^T = \mathcal{V}^T\mathcal{U}. \quad (\text{A11})$$

Note that in this representation, the matrix \mathcal{M} is no longer real matrix in general. However, this representation is suitable for describing the quantum dynamics of the two-component BEC.

APPENDIX B: EXPLICIT EXPRESSION OF \mathcal{U}_0

In this Appendix, we will give the explicit expression of \mathcal{U}_0 of the matrix $U_0 = e^{\frac{1}{2}(\eta_{ij}Y^{ij} + \eta_{ij}^*Y_{ij})}$. The explicit form of the matrix generators $\{Y_{ij}, Y^{ij}, Y_l^k\}$ is [59]

$$\begin{aligned} (\kappa Y_{ij})_{ab} &= \delta_{a,2+i}\delta_{b,j} + \delta_{a,2+j}\delta_{b,i}, \\ (\kappa Y^{ij})_{ab} &= \delta_{a,i}\delta_{b,2+j} + \delta_{a,j}\delta_{b,2+i}, \\ (\kappa Y_l^k)_{ab} &= \delta_{a,k}\delta_{b,l} + \delta_{2+k,b}\delta_{2+l,a}, \end{aligned} \quad (\text{B1})$$

where $\kappa = \text{diag}(1, 1, -1, -1)$. Then, we define

$$\mathcal{A} = \frac{1}{2}\eta_{ij}Y^{ij} + \frac{1}{2}\eta_{ij}^*Y_{ij} = \begin{pmatrix} 0 & \eta \\ -\eta^* & 0 \end{pmatrix}. \quad (\text{B2})$$

According to the authors of Ref. [46], its eigenvalues are of the form $\{\lambda_+, \lambda_-, -\lambda_+, -\lambda_-\}$, where

$$\lambda_{\pm} = \frac{1}{2}\sqrt{\text{Tr}(\mathcal{A}^2) \pm \sqrt{\text{Tr}(\mathcal{A}^2)^2 - 16\det(\mathcal{A})}}. \quad (\text{B3})$$

It can be calculated directly by MATHEMATICA that \mathcal{U}_0 is given as

$$\begin{aligned} \mathcal{U}_{0,11} &= \frac{|\eta_{11}|^2 - |\eta_{22}|^2}{2(\lambda_+^2 - \lambda_-^2)} [\cos(\lambda_-) - \cos(\lambda_+)] + \frac{1}{2} [\cos(\lambda_-) + \cos(\lambda_+)], \\ \mathcal{U}_{0,12} &= \frac{\eta_{11}\eta_{12}^* + \eta_{22}^*\eta_{12}}{\lambda_+^2 - \lambda_-^2} [\cos(\lambda_-) - \cos(\lambda_+)], \\ \mathcal{U}_{0,21} &= \frac{\eta_{11}^*\eta_{12} + \eta_{22}\eta_{12}^*}{\lambda_+^2 - \lambda_-^2} [\cos(\lambda_-) - \cos(\lambda_+)], \\ \mathcal{U}_{0,22} &= -\frac{|\eta_{11}|^2 - |\eta_{22}|^2}{2(\lambda_+^2 - \lambda_-^2)} [\cos(\lambda_-) - \cos(\lambda_+)] + \frac{1}{2} [\cos(\lambda_-) + \cos(\lambda_+)]. \end{aligned} \quad (\text{B4})$$

If \mathcal{U}_0 is Hermitian, $\mathcal{U}_{0,11}$ and $\mathcal{U}_{0,22}$ should be real, meanwhile $\mathcal{U}_{0,12} = \mathcal{U}_{0,21}^*$. These conditions lead to that $\cos(\lambda_+)$, $\cos(\lambda_-)$, and

$\lambda_+^2 - \lambda_-^2$ should be real numbers. On the other hand, from Eq. (B3), we have

$$\begin{aligned}
\lambda_+^2 - \lambda_-^2 &= \frac{1}{2} \sqrt{\text{Tr}(\mathcal{A}^2)^2 - 16 \det(\mathcal{A})} \\
&= \frac{1}{2} \sqrt{4(|\eta_{11}|^2 + |\eta_{22}|^2 + 2|\eta_{12}|^2)^2 - 16|\eta_{12}^2 - \eta_{11}\eta_{22}|^2} \\
&= \sqrt{(\eta_{11}^2 + |\eta_{22}|^2 + 2|\eta_{12}|^2 + 2|\eta_{12}^2 - \eta_{11}\eta_{22}|)(\eta_{11}^2 + |\eta_{22}|^2 + 2|\eta_{12}|^2 - 2|\eta_{12}^2 - \eta_{11}\eta_{22}|)} \\
&\geq \sqrt{(\eta_{11}^2 + |\eta_{22}|^2 + 2|\eta_{12}|^2 + 2|\eta_{12}^2 - \eta_{11}\eta_{22}|)(\eta_{11}^2 + |\eta_{22}|^2 + 2|\eta_{12}|^2 - 2|\eta_{12}|^2 - 2|\eta_{11}||\eta_{22}|)} \\
&= \sqrt{(\eta_{11}^2 + |\eta_{22}|^2 + 2|\eta_{12}|^2 + 2|\eta_{12}^2 - \eta_{11}\eta_{22}|)(\eta_{11}^2 - |\eta_{22}|^2)^2} \\
&\geq 0.
\end{aligned} \tag{B5}$$

Hence, $\lambda_+^2 - \lambda_-^2$ is real. Meanwhile, since $\text{Tr}(\mathcal{A}^2) = -2(|\eta_{11}|^2 + |\eta_{22}|^2 + 2|\eta_{12}|^2)$, according to Eq. (B3), both λ_+ and λ_- are imaginary. Thus, $\cos(\lambda_+)$ and $\cos(\lambda_-)$ are real. Hence, the conditions of \mathcal{U}_0 being Hermitian are all satisfied. As a result, we prove that \mathcal{U}_0 is a 2×2 Hermitian matrix.

-
- [1] I. Bloch, Ultracold quantum gases in optical lattices, *Nat. Phys.* **1**, 23 (2005).
- [2] I. Bloch, J. Dalibard, and W. Zwerger, Many-body physics with ultracold gases, *Rev. Mod. Phys.* **80**, 885 (2008).
- [3] C. Chin, R. Grimm, P. Julienne, and E. Tiesinga, Feshbach resonances in ultracold gases, *Rev. Mod. Phys.* **82**, 1225 (2010).
- [4] L. W. Clark, A. Gaj, L. Feng, and C. Chin, Collective emission of matter-wave jets from driven Bose–Einstein condensates, *Nature (London)* **551**, 356 (2017).
- [5] L. Feng, J. Hu, L. W. Clark, and C. Chin, Correlations in high-harmonic generation of matter-wave jets revealed by pattern recognition, *Science* **363**, 521 (2019).
- [6] H. Fu, L. Feng, B. M. Anderson, L. W. Clark, J. Hu, J. W. Andrade, C. Chin, and K. Levin, Density waves and jet emission asymmetry in Bose fireworks, *Phys. Rev. Lett.* **121**, 243001 (2018).
- [7] L. W. Clark, L.-C. Ha, C.-Y. Xu, and C. Chin, Quantum dynamics with spatiotemporal control of interactions in a stable Bose-Einstein condensate, *Phys. Rev. Lett.* **115**, 155301 (2015).
- [8] L. W. Clark, L. Feng, and C. Chin, Universal space-time scaling symmetry in the dynamics of bosons across a quantum phase transition, *Science* **354**, 606 (2016).
- [9] L. Feng, L. W. Clark, A. Gaj, and C. Chin, Coherent inflationary dynamics for Bose–Einstein condensates crossing a quantum critical point, *Nat. Phys.* **14**, 269 (2018).
- [10] H. Fu, Z. Zhang, K.-X. Yao, L. Feng, J. Yoo, L. W. Clark, K. Levin, and C. Chin, Jet substructure in fireworks emission from nonuniform and rotating Bose-Einstein condensates, *Phys. Rev. Lett.* **125**, 183003 (2020).
- [11] Z. Zhang, K.-X. Yao, L. Feng, J. Hu, and C. Chin, Pattern formation in a driven Bose–Einstein condensate, *Nat. Phys.* **16**, 652 (2020).
- [12] J. Hu, L. Feng, Z. Zhang, and C. Chin, Quantum simulation of Unruh radiation, *Nat. Phys.* **15**, 785 (2019).
- [13] Y.-Y. Chen, P. Zhang, W. Zheng, Z. Wu, and H. Zhai, Many-body echo, *Phys. Rev. A* **102**, 011301(R) (2020).
- [14] C. Lv, R. Zhang, and Q. Zhou, SU(1, 1) echoes for breathers in quantum gases, *Phys. Rev. Lett.* **125**, 253002 (2020).
- [15] C. Lyu, C. Lv, and Q. Zhou, Geometrizing quantum dynamics of a Bose-Einstein condensate, *Phys. Rev. Lett.* **125**, 253401 (2020).
- [16] J. Zhang, X. Yang, C. Lv, S. Ma, and R. Zhang, Quantum dynamics of cold atomic gas with SU(1,1) symmetry, *Phys. Rev. A* **106**, 013314 (2022).
- [17] Y. Cheng and Z.-Y. Shi, Many-body dynamics with time-dependent interaction, *Phys. Rev. A* **104**, 023307 (2021).
- [18] E. L. Hahn, Spin echoes, *Phys. Rev.* **80**, 580 (1950).
- [19] T.-L. Ho, Spinor Bose condensates in optical traps, *Phys. Rev. Lett.* **81**, 742 (1998).
- [20] Y. Kawaguchi and M. Ueda, Spinor Bose–Einstein condensates, *Phys. Rep.* **520**, 253 (2012).
- [21] T. Ohmi and K. Machida, Bose-Einstein condensation with internal degrees of freedom in alkali atom gases, *J. Phys. Soc. Jpn.* **67**, 1822 (1998).
- [22] C. J. Myatt, E. A. Burt, R. W. Ghrist, E. A. Cornell, and C. E. Wieman, Production of two overlapping Bose-Einstein condensates by sympathetic cooling, *Phys. Rev. Lett.* **78**, 586 (1997).
- [23] D. S. Hall, M. R. Matthews, J. R. Ensher, C. E. Wieman, and E. A. Cornell, Dynamics of component separation in a binary mixture of Bose-Einstein condensates, *Phys. Rev. Lett.* **81**, 1539 (1998).
- [24] D. S. Hall, M. R. Matthews, C. E. Wieman, and E. A. Cornell, Measurements of relative phase in two-component Bose-Einstein condensates, *Phys. Rev. Lett.* **81**, 1543 (1998).
- [25] G. Modugno, M. Modugno, F. Riboli, G. Roati, and M. Inguscio, Two atomic species superfluid, *Phys. Rev. Lett.* **89**, 190404 (2002).
- [26] S. B. Papp, J. M. Pino, and C. E. Wieman, Tunable miscibility in a dual-species Bose-Einstein condensate, *Phys. Rev. Lett.* **101**, 040402 (2008).
- [27] G. Thalhammer, G. Barontini, L. De Sarlo, J. Catani, F. Minardi, and M. Inguscio, Double species Bose-Einstein condensate with tunable interspecies interactions, *Phys. Rev. Lett.* **100**, 210402 (2008).

- [28] D. J. McCarron, H. W. Cho, D. L. Jenkin, M. P. Köppinger, and S. L. Cornish, Dual-species Bose-Einstein condensate of ^{87}Rb and ^{133}Cs , *Phys. Rev. A* **84**, 011603(R) (2011).
- [29] A. D. Lercher, T. Takekoshi, M. Debatin, B. Schuster, R. Rameshan, F. Ferlaino, R. Grimm, and H. C. Nägerl, Production of a dual-species Bose-Einstein condensate of Rb and Cs atoms, *Eur. Phys. J. D* **65**, 3 (2011).
- [30] B. Pasquiou, A. Bayerle, S. M. Tzanova, S. Stellmer, J. Szczechowski, M. Parigger, R. Grimm, and F. Schreck, Quantum degenerate mixtures of strontium and rubidium atoms, *Phys. Rev. A* **88**, 023601 (2013).
- [31] L. Wacker, N. B. Jørgensen, D. Birkmose, R. Horchani, W. Ertmer, C. Klempt, N. Winter, J. Sherson, and J. J. Arlt, Tunable dual-species Bose-Einstein condensates of ^{39}K and ^{87}Rb , *Phys. Rev. A* **92**, 053602 (2015).
- [32] F. Wang, X. Li, D. Xiong, and D. Wang, A double species ^{23}Na and ^{87}Rb Bose-Einstein condensate with tunable miscibility via an interspecies Feshbach resonance, *J. Phys. B: At. Mol. Opt. Phys.* **49**, 015302 (2016).
- [33] A. Trautmann, P. Ilzhöfer, G. Durastante, C. Politi, M. Sohmen, M. J. Mark, and F. Ferlaino, Dipolar quantum mixtures of Erbium and Dysprosium atoms, *Phys. Rev. Lett.* **121**, 213601 (2018).
- [34] T.-L. Ho and V. B. Shenoy, Binary mixtures of Bose condensates of alkali atoms, *Phys. Rev. Lett.* **77**, 3276 (1996).
- [35] B. D. Esry, C. H. Greene, J. P. Burke and J. L. Bohn, Hartree-Fock theory for double condensates, *Phys. Rev. Lett.* **78**, 3594 (1997).
- [36] O. E. Alon, A. I. Streltsov, and L. S. Cederbaum, Multi-configurational time-dependent Hartree method for bosons: Many-body dynamics of bosonic systems, *Phys. Rev. A* **77**, 033613 (2008).
- [37] P. Ao and S. T. Chui, Binary Bose-Einstein condensate mixtures in weakly and strongly segregated phases, *Phys. Rev. A* **58**, 4836 (1998).
- [38] J. I. Cirac, M. Lewenstein, K. Mølmer, and P. Zoller, Quantum superposition states of Bose-Einstein condensates, *Phys. Rev. A* **57**, 1208 (1998).
- [39] K. M. Mertes, J. W. Merrill, R. Carretero-González, D. J. Frantzeskakis, P. G. Kevrekidis, and D. S. Hall, Nonequilibrium dynamics and superfluid ring excitations in binary Bose-Einstein condensates, *Phys. Rev. Lett.* **99**, 190402 (2007).
- [40] H. Pu and N. P. Bigelow, Properties of two-species Bose condensates, *Phys. Rev. Lett.* **80**, 1130 (1998).
- [41] E. Timmermans, Phase separation of Bose-Einstein condensates, *Phys. Rev. Lett.* **81**, 5718 (1998).
- [42] A. Micheli, D. Jaksch, J. I. Cirac, and P. Zoller, Many-particle entanglement in two-component Bose-Einstein condensates, *Phys. Rev. A* **67**, 013607 (2003).
- [43] S. Tojo, Y. Taguchi, Y. Masuyama, T. Hayashi, H. Saito, and T. Hirano, Controlling phase separation of binary Bose-Einstein condensates via mixed-spin-channel Feshbach resonance, *Phys. Rev. A* **82**, 033609 (2010).
- [44] M. Trippenbach, K. Góral, K. Rzazewski, B. Malomed, and Y. B. Band, Structure of binary Bose-Einstein condensates, *J. Phys. B: At. Mol. Opt. Phys.* **33**, 4017 (2000).
- [45] C. Wang, C. Gao, C.-M. Jian, and H. Zhai, Spin-orbit coupled spinor Bose-Einstein condensates, *Phys. Rev. Lett.* **105**, 160403 (2010).
- [46] C.-Y. Wang and Y. He, The quantum dynamics of two-component Bose-Einstein condensate: An $\text{Sp}(4, R)$ symmetry approach, *J. Phys.: Condens. Matter* **34**, 455401 (2022).
- [47] A. Perelomov, *Generalized Coherent States and Their Applications* (Springer, Berlin, 1986).
- [48] C. Weedbrook, S. Pirandola, R. García-Patrón, N. J. Cerf, T. C. Ralph, J. H. Shapiro, and S. Lloyd, Gaussian quantum information, *Rev. Mod. Phys.* **84**, 621 (2012).
- [49] R. Simon, Peres-horodecki separability criterion for continuous variable systems, *Phys. Rev. Lett.* **84**, 2726 (2000).
- [50] R. Simon, E. C. G. Sudarshan, and N. Mukunda, Gaussian pure states in quantum mechanics and the symplectic group, *Phys. Rev. A* **37**, 3028 (1988).
- [51] T. Colas, J. Grain, and V. Vennin, Four-mode squeezed states: Two-field quantum systems and the symplectic group $\text{Sp}(4, \mathbb{R})$, *Eur. Phys. J. C* **82**, 6 (2022).
- [52] Y. Alhassid, F. Gürsey, and F. Iachello, Group theory approach to scattering, *Ann. Phys. (NY)* **148**, 346 (1983).
- [53] J. Deenen and C. Quesne, Boson representations of the real symplectic group and their applications to the nuclear collective model, *J. Math. Phys.* **26**, 2705 (1985).
- [54] M. Enayati, J.-P. Gazeau, M. A. del Olmo, and H. Pejhan, Anti-de Sitterian "massive" elementary systems and their Minkowskian and Newtonian limits, [arXiv:2307.06690](https://arxiv.org/abs/2307.06690).
- [55] V. Penna and A. Richaud, Two-species boson mixture on a ring: A group-theoretic approach to the quantum dynamics of low-energy excitations, *Phys. Rev. A* **96**, 053631 (2017).
- [56] A. Richaud and V. Penna, Quantum dynamics of bosons in a two-ring ladder: Dynamical algebra, vortexlike excitations, and currents, *Phys. Rev. A* **96**, 013620 (2017).
- [57] C. Charalambous, M. Á. García-March, G. Muñoz-Gil, P. R. Grzybowski, and M. Lewenstein, Control of anomalous diffusion of a Bose polaron, *Quantum* **4**, 232 (2020).
- [58] L. Pitaevskii and S. Stringari, *Bose-Einstein Condensation and Superfluidity* (Oxford University Press, New York, 2016).
- [59] K. Hasebe, $\text{Sp}(4; R)$ squeezing for Bloch four-hyperboloid via the non-compact Hopf map, *J. Phys. A: Math. Theor.* **53**, 055303 (2020).
- [60] D. J. Rowe, G. Rosensteel, and R. Gilmore, Vector coherent state representation theory, *J. Math. Phys.* **26**, 2787 (1985).
- [61] R. Coquereaux and A. Jadczyk, Conformal theories, curved phase spaces, relativistic wavelets and the geometry of complex domains, *Rev. Math. Phys.* **02**, 1 (1990).
- [62] C. V. Parker, L.-C. Ha, and C. Chin, Direct observation of effective ferromagnetic domains of cold atoms in a shaken optical lattice, *Nat. Phys.* **9**, 769 (2013).
- [63] V. Galitski and I. B. Spielman, Spin orbit coupling in quantum gases, *Nature (London)* **494**, 49 (2013).